
Article:
Carcadea, E., Ismail, M.S., Ingham, D.B. et al. (6 more authors) (2021) Effects of geometrical dimensions of flow channels of a large-active-area PEM fuel cell: A CFD study. International Journal of Hydrogen Energy, 46 (25). pp. 13572-13582. ISSN 0360-3199

https://doi.org/10.1016/j.ijhydene.2020.08.150

Effects of geometrical dimensions of flow channels of a large-active-area PEM fuel cell: a CFD study

E. Carcadea[a*], M.S. Ismail[b], D.B. Ingham[b], L. Patularu[a], D. Schitea[a], A. Marinoiu[a], D. Ebrasu[a], D. Mocanu[a] and M. Varlam[a]

[a]National Research and Development Institute for Cryogenics and Isotopic Technologies - ICSI Rm. Valcea, 240050, Romania

[b]Energy2050, Department of Mechanical Engineering, Faculty of Engineering, University of Sheffield, Sheffield S10 2TN, UK

(*) elena.carcadea@icsi.ro

Abstract

Various flow field designs have been numerically investigated to evaluate the effect of pattern and the cross-sectional dimensions of the channel on the performance of a large active area PEM fuel cell. Three types of multiple-serpentine channels (7-channels, 11-channels and 14-channels) have been chosen for the 200 cm^2 fuel cell investigated and numerically analysed by varying the width and the land of the channel. The CFD simulations showed that as the channel width decreases, as in the 14-channels serpentine case, the performance improves, especially at high current densities where the concentration losses are dominant. The optimum configuration, i.e. the 14-channels serpentine, has been manufactured and tested experimentally and a very good agreement between the experimental and modelling data was achieved. 4 channel depths have been considered (0.25, 0.4, 0.6 and 0.8 mm) in the CFD study to determine ~~and~~ the effects on the pressure drop and water content ~~is described~~. Up to 7 % increase in the maximum reported current density has been achieved for the smallest depth and this due to the better removal of excess liquid water and better humidification of the membrane. Also, the influence of the air flow rate has been evaluated: the current density at 0.6V increased by around 25% when air flow rate was increased 4 times; this is attributed to better removal of excess liquid water.

Keywords: PEM fuel cell; numerical model; flow field design; water management; large active area; performance improvement.

1. Introduction

Hydrogen and fuel cells have paved the way for integrated energy systems that concomitantly approach the main energy and environmental challenges and have the versatility to adapt to the various renewable and intermittent energy sources that are existing worldwide. Although a significant amount of research has been carried out in the last decades in the fuel cell domain and successful demonstration projects are available [1], there is still a large demand to sustain the development of this technology. Enhanced products due to improved designs of some of the component (catalyst, membrane, gas diffusion layer and bipolar plate) and the system level are required to meet the performance, durability and cost targets [2], in order for fuel cells to become competitive for automotive, portable and stationary applications against the current available solutions. The Fuel Cell and Hydrogen Joint Undertaking (FCH JU) vision for 2030 points out that for driving down the costs, while keeping an acceptable level of performance and durability, it is necessary to progress at a lab-scale level to achieve fundamental improvements in all the components of the fuel cell.

Design parameters, such as flow field pattern or channel dimensions (width, depth), are key factors for Proton Exchange Membrane Fuel Cells operation due to their impact on the performance and durability. A good distribution and uniformity of reacting species, without dead zones, minimization of the pressure loss or a better water and heat management are just a few critical challenges that can be addressed by flow field design optimization [3-9]. Without control, a variation in the water generation and elimination can occur and both of the consequences (i.e. dehydration or flooding) have a very harmful effect on the performance [10]. One of the key component, the membrane electrolyte, requires water in order to exhibit good protonic conductivity, but in the other layers of the fuel cell, the amount of liquid water should be kept to the minimum. Liquid water must

be prevented from accumulating on the electrode surfaces, in the pores of the gas diffusion layer, and in the fluid flow fields. The presence of liquid water in these regions will hinder the diffusion of reactants to the catalyst active sites, thus degrading the performance [11-12]. An effective water management will control and adjust the transport of water in such a way that a sufficient amount of water is maintained in the proton conductive phases, and the excess liquid water will be purged from the cell with the same rate as it is produced, with minimum blockage of the gas transport paths.
Several channel configurations (serpentine ~~[13-15, 28]~~[13-17], parallel ~~[16,30]~~ [18-20], interdigitated [21], pin type or combinations ~~[18-19, 26]~~ [22-26]) or channel to land sizes have been employed so far in numerical and experimental investigations for enhancing the PEM fuel cell overall performance. Each configuration has pros and cons related to the phenomena taking place inside the fuel cell layers, the mass and heat transport challenges being the most frequently reported. Pin type or parallel channels feature a lower pressure drop but an uneven distribution of reactants and products, resulting in the stagnation of water. Lim et al. [20] proposed a modified parallel flow field which was found to: overcome the latter drawbacks, increase the uniformity of the distribution of the current density, and improve cell performance due to better supply of reacting gases and improved removal of excess liquid water. A relatively large pressure drop, featured by serpentine channels, can effective eliminate the liquid water collected in the flow fields but leads to use of higher pumping power. The relatively low pressure drop can be realised in parallel flow channels, but they are prone to flooding [7]. By replacing the channels with open pore cellular foam, as in the research of Wilberforce et al. [25], pressure drop is minimised and the cell performance is doubled compared with those of the serpentine flow channels. On the other hand, the serpentine channels demonstrate a larger pressure drop [27] due to the larger channel length, although flooding can appear in the bending zones. As regards to the channel to land ratio, channel cross-section dimensions (i.e. width and depth) and cross section design (e.g. rectangular, trapezoidal, triangular and curved), there are several studies that have investigated the influence of the above-mentioned factors on some local transport phenomena that can affect the fuel cell performance: under land convection [7], distribution of reactant and temperature ~~[18]~~ [22] and, dynamics of liquid water ~~[28]~~ [16]. The channel-to-land ratio larger than 1 (meaning channel width larger than land width) is recommended for efficient water removal, effective transport of the reactants to the gas diffusion layers and ultimately reduced voltage losses; however, mechanical instability (the bulge of gas diffusion layers into the channels) and poor thermal and electrical contacts [7,12] are potential issues with high channel-to-land ratios.

Among several types of design for flow channels, the multiple serpentine-parallel channels ~~[10, 22, 37-38]~~ [10, 28-30] have proved to be one of the most effective designs for the removal of liquid water, especially for fuel cells with large sizes of the active areas.

The scaling up of PEM fuel cells has led to disputed conclusions. In the study of Vijayakrishnan ~~[36]~~ [31] it was concluded that by scaling up the PEM fuel cell geometry, from 25 cm^2 to 70 cm^2, the performance decreases, this being also valid in ~~[38]~~ [30] where the cross flow and triple serpentine channels have been investigated and a reduction in performance was achieved by scaling up the geometry from 50 to 200 cm^2. In another publication ~~[20]~~ [32] the performance did not suffer a decrease and contrarily an improvement was achieved by increasing the active area of the cell from 50 to 441 cm^2, in case of an adequate water management is achieved. The present investigation of a 200 cm^2 active area fuel cell is considered adequate for fuel cell developers and integrators, far exceeding the area of 1 to 25 cm^2 used in research laboratories for materials development, as well as areas of around 100 cm^2 used in demonstration projects. The advantages of using 200 cm^2 fuel cells comes from the variety of applications that can integrate such large-scale electrochemical devices, from stationary, portable to automotive applications. There are numerous challenges in the scaling-up of the PEM fuel cell ~~[21, 36-37]~~ [31, 33-35], of which the mass transport limitations are the key challenges due to their detrimental effect on the performance and durability. The present work numerically investigates a large size PEM fuel cell used in a stack of a micro-grid application~~, an exploded view of the cell with some of the components is presented in Fig. 1.~~ Based on previous results, an extension of the lab scale (5 cm^2) fuel cell ~~[29]~~ [36] and medium scale demonstration project (44 cm^2) fuel cell ~~[30]~~ [19] to the real size PEM fuel cell is done in order to investigate critical issues that can affect the cell performance and can have a detrimental effect on its operation.

Although a significant number of fuel cell models have been developed so far by various research teams [13-14, ~~23, 31-32,~~ 37-39] and some CFD vendors ~~[33]~~ [40], there is still a need for a comprehensive model to better understand the parameters affecting the performance and to enable more-informed scaling-up of PEM fuel cells ~~[36]~~ [31]. Two design methods of the flow-field design have been considered in this study: the pattern of the flow channels and the cross-sectional dimensions (i.e. the width and the depth) of the flow channels. The effects of other detailed chemistry and electrochemistry processes, charge transport, heat and water generation are taken into account and are based on optimized values obtained in previous investigations ~~[29]~~ [36]. The numerical results are validated against experimental data for an optimum pattern fuel cell that have been manufactured (14-channels serpentine configuration) and a good agreement was found, revealing that CFD can be a powerful modelling tool that can lead to improvements in performance and a reduction in the time and costs required for experiments. Such investigations can move forward the scale-up of the fuel cell manufacturing lines from small to large size fuel cells.

2. Mathematical Model and Numerical Implementation

The mathematical model used to analyse the effects of geometrical dimensions of the flow channels on a large active area PEM fuel cell performance is three-dimensional, non-isothermal and deals with multi-physics and multi-phase flows. The conservation equations for mass, momentum, species, charge and energy are taken into consideration, and the ANSYS Fluent solver with the PEM Fuel Cell Module ~~[33]~~ [40] has been used based on some assumptions and boundary conditions. The Gauss-Seidel method was chosen for solving the system of equations applied to describe the PEM fuel cell operation.

A comprehensive mathematical model with all conservation equations that describe the PEM fuel cell operation has been presented in previous works ~~[29-30]~~ [19, 36], therefore it will not be repeated here. However, for the convenience of readers, a brief model description is given hereafter: the mass, momentum, species, charge and energy conservation equations are solved for understanding the effect of the geometrical design on the complex phenomena that take place in fuel cells, and consequently on the performance. Source terms are included in the transport equations to account for the electrochemical reactions (species diffusion, consumption, generation), for the effects of the porous media, for heat generation and for implementing changes in material properties and common boundary conditions. Steady state conditions, non-isothermal operation, ideal gas mixtures, laminar flow, isotropic and homogenous components are considered in this study. The water existing in different forms, as gas, liquid or in dissolved state, as well as the effect of the catalyst complex microstructure have been taken into consideration in our previous model and are used as inputs in this study. The aim is to comprehensively investigate the water management influence on a large active area PEM fuel cell performance.

The boundary conditions prescribed for solving the conservation equations are only for the external surfaces, the fuel cell being treated as a single domain. Accordingly, Dirichlet boundary conditions are used for gas flow inlets: mass flow rate, species mass fractions and temperature. Potentiostatic boundary conditions have been used for the external walls, the anode wall being grounded to zero volts and the cathode terminal wall to a constant voltage with the maximum value equal to the open circuit value. After assigning relevant values for the operating conditions and material properties, as in Tables 1 and 2, the flow is initialized and the simulation starts. It is recommend to start with a high voltage, close to the open circuit voltage, and then to use steps of 0.05–0.1 volts between each converged solution. An average current density is calculated at both the anode and the cathode catalyst layers for each iteration. If the difference between these values is less than 10^{-4} and the residuals for the other scalar variables considered in the model fall to a small value (i.e. 10^{-6}) then the iterations will stop and the solution is considered convergent. For convergence problems, it is recommended to decrease the under-relaxation factors for the transport equations to values that do not affect the accuracy of the results.

Table 1. The physical parameters used in the model ~~[29, 30]~~ [19, 36].

Parameter	Value	Unit
GDL/MPL/CL porosity (ε)	0.7/0.6/0.5	-
GDL/MPL/CL permeability (K)	$3\times10^{-12}/1\times10^{-12}/2\times10^{-13}$	m^2
Anodic reference exchange current density (j_a^{ref})	10000	A/m^2
Cathodic reference exchange current density (j_c^{ref})	1	A/m^2
GDL/MPL/CL contact angle (θ_c)	110/130/95	o
Open circuit voltage (V_{oc})	0.962	V
Membrane thickness	14	µm
GDL thickness	255	µm
MPL thickness	25	µm
Anode/ Cathode Catalyst layer thickness	5/12	µm
Dry membrane density (ρ_i)	2000	kg/m^3
Equivalent weight of the membrane (EW)	1100	kg/kmol

Table 2. The boundary conditions used in the model ~~[29, 30]~~ [19, 36].

Parameter	Value	Unit
Anodic mass flow rate at inlet	8×10^{-6}	kg/s
Cathodic mass flow rate at inlet	1.1×10^{-4}	kg/s
H_2 mass fraction at anode inlet	0.554	-
H_2O mass fraction for at anode inlet	0.446	-
O_2 mass fraction for at cathode inlet	0.22	-
H_2O mass fraction for at cathode inlet	0.053	-
Relative humidity at anode/cathode inlets	80 %	-
Temperature at anode/cathode inlets	55	°C

The ANSYS Fluent 2019 R3 has been utilized to investigate the geometrical design influence on the water management and performance of fuel cells. The base case parameters, operating and boundary conditions as presented in Tables 1 and 2 have been used in all cases simulated, unless otherwise specified. Polarization curves are obtained after running the simulations, one simulation giving one point from the polarization curve. A High Performance Computer (HPC) with 32 processes and 64 GB of RAM shared on 2 workstations have been used for the parallel processing of the cases investigated in order to reduce the time required for obtaining a converged solution. Approximatively 3 hours it takes to obtain 1 point on the polarization curve, using parallel processing.

The computational geometries have been built using the Gambit® 2.4.6 pre-processing software and the grid-independent solution have been found for all fuel cells investigated. 3 patterns based on the serpentine configuration have been used (7-channels, 11-channels and 14-channels) and 4 depths (0.25, 0.4, 0.6 and 0.8 mm). The mesh for all cases investigated is between 4.8 and 6.4 million elements and this ensures the mesh-independent solutions, the case with 14-channels serpentine PEM fuel cell is showed in Fig. ~~2~~ 1. The sizes and the design of the 200 cm^2 fuel cell are comparable with those of a real fuel cell. The same configuration for the anode and cathode channels have been used, the patterns and sizes of the configurations investigated are presented in Table 3. Also, the contact area between the bipolar plate (BP) and gas diffusion layer (GDL) is reported. Also, the contact area between the bipolar plate (BP) and gas diffusion layer (GDL) is reported. The BP ~~bipolar plate~~ is 200 mm × 100 mm in the x- and y– directions and its thickness depends on the channel depth.

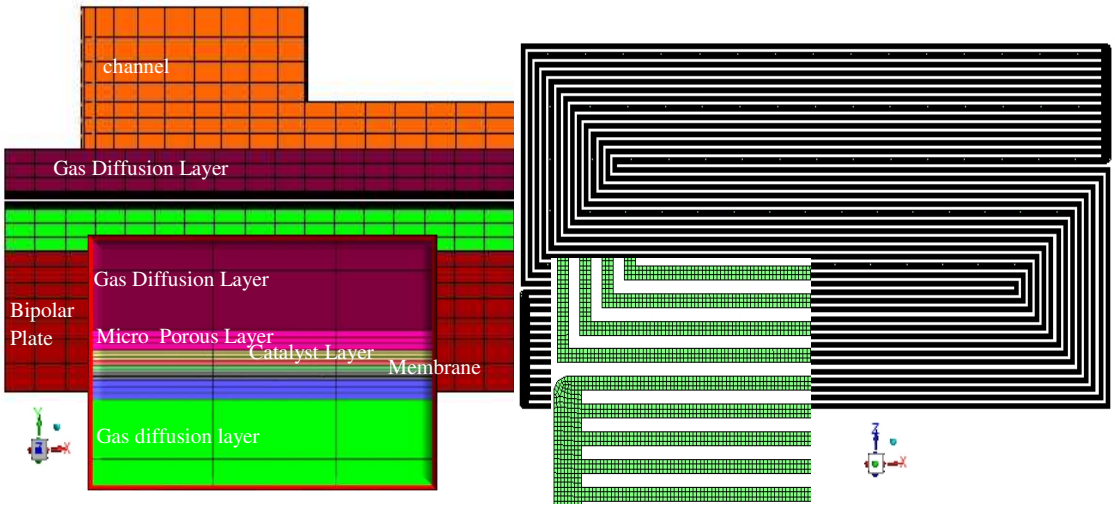

Fig. 1 – PEM fuel cell computational mesh in the cross section (x-y) and flow direction (x-z) for 14-channels serpentine configuration.

Regarding the numerical methods and the interpolation schemes used in the CFD investigations, it is known that a converged and mesh-independent solution of a well-posed problem will provide helpful results only if an appropriate setup is chosen. Higher-order interpolation schemes, such as the second-order upwind and QUICK, offer improved accuracy for the numerical simulations, therefore a second-order upwind scheme has been used in all the simulations.

Table 3 Patterns and sizes of the flow field channels investigated.

Pattern	Channel width	Land width	Channel depth	Contact area between GDL-BP
7-channels serpentine	2.4 mm	2.4 mm	0.6 mm (base case)	99,81 cm^2
11-channels serpentine	1.6 mm	1.4 mm	0.6 mm (base case)	100,95 cm^2
14-channels serpentine	1.2 mm	1.2 mm	0.25 mm	104,81 cm^2
			0.4 mm	
			0.6 mm (base case)	
			0.8 mm	

3. Results and Discussions

A computational fluid dynamics (CFD) investigation based on the ANSYS Multiphysics software and PEM Fuel Cell Module have been applied to analyse the impact of the flow field pattern and dimensions on a 200 cm^2 PEM fuel cell performance. 3 patterns for the fluid flow channels have been used in the numerical investigation, namely: a 7-channels serpentine, an 11-channels serpentine and a 14-channels serpentine. The optimum pattern has been used further to analyse the effect of the channel depth on the water management and accordingly on the PEM fuel cell performance. Also, the sensitivity of the mass transport limitations to air mass flow rate is discussed.

3.1 Model Validation

A comparison between the numerical results and experimental data was performed to validate the model. For numerical model, the 14-channels serpentine fuel cell with 0.6 mm channel depth and 1.2 mm land and channel width have been used as a base case. The 200 cm^2 PEM fuel cell adopted in

the experimental investigations and the test station were developed in-house, see Fig. ~~3~~ 2. The test station used for experiments has a power range between 1-1500 watts and fully adjustable working parameters (stoichiometry, pressures, humidity, and temperature). It includes: gas heated lines to prevent water condensation, back-pressure regulators and mass flow controllers, pressure valves and sensors, bubble humidifiers with an adaptable water level and temperature for humidifying the air and hydrogen streams up to 99% RH and dew point up to 65°C, and an electronic load for simulating the operating conditions. The polarisation curve of the fuel cell was obtained using a PLA800 60-300 electrical load bridge by applying various cell potentials in the range of the open circuit voltage (0.962 V) and 0.4 V, thus determining the corresponding currents. At each current point, the stoichiometry of gases was calculated using Faradaic low and used to set the mass flow controllers. The stoichiometric coefficients used in the experiments for hydrogen and air were 1.2 and 2.5, respectively.

A membrane electrode assembly (MEA), developed by HyPlat in South Africa, has been used in the experiments. This MEA was based on a 100 mm x 200 mm GDL from Freudenberg GmbH, H23C9 type, and incorporates an 18µm thin Gore M735.18 membrane, with 0.1 and 0.4 mg/cm^2 Pt loadings in the anode and cathode catalyst layers. The fuel cell set up has two 32 mm thick fiberglass high strength end plates that incorporates 2mm gold coated cooper plates for current collecting. The anode and cathode flow fields were CNC machined into graphite plates from IRD FuelCells Denmark.

To validate the numerical model, a comparison of the polarization curves obtained experimentally and numerically have been performed. A good agreement between the two sets of results was obtained, the trend of the modelling data follow that of the experimental data; see Fig. ~~4~~ 3.

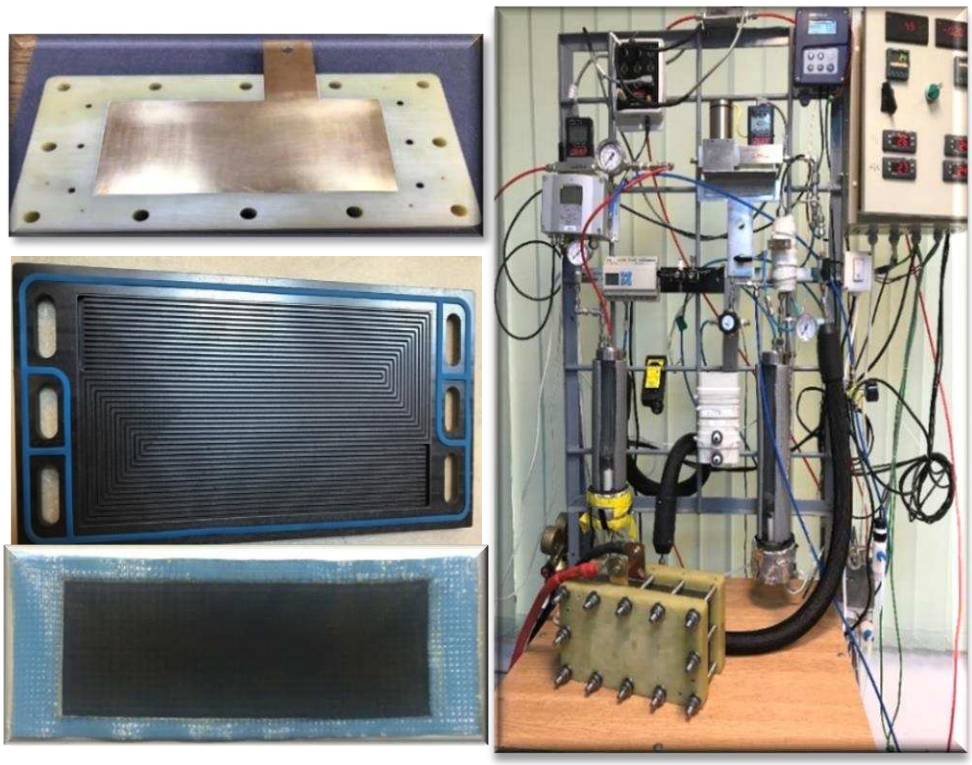

Fig. ~~3~~ 2 – The fuel cell components: collector plate (top left), bipolar plate (medium left) and MEA with gasket (bottom left), and the test station used in experiments (right).

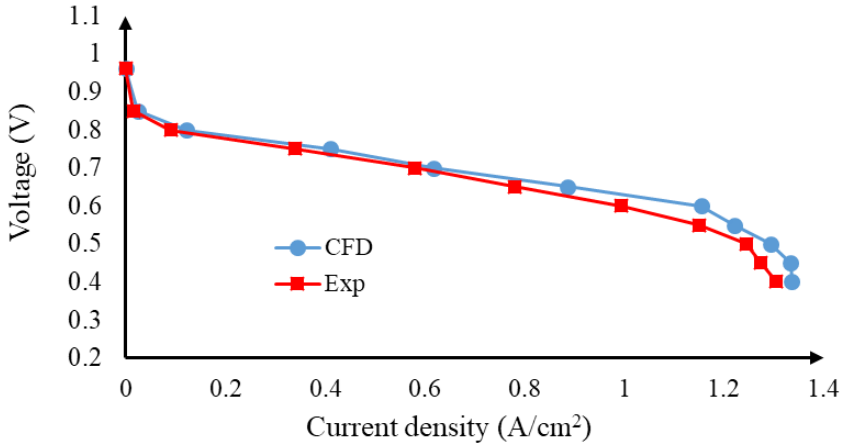

Fig. ~~4~~ 3 – The polarisation curves of the 14-channels serpentine fuel cell: experimental and simulated

3.2. Influence of the flow channels pattern

The CFD model has been used to analyse the impact of the flow channels pattern on the fuel cell performance. Serpentine configurations with multiple channels have been considered for the 200 cm^2 fuel cells; the aim was to ensure a balance between the electrical conductivity requirement and gas transport efficiency. Therefore, three configurations have been obtained, namely: a 7-channels serpentine, an 11- channels serpentine and a 14- channels serpentine, as a result of the variation of the widths of both the flow channel and land; see Table 3. By decreasing the channels width from 2.4 mm to 1.2 mm an improvement of the performance has been achieved starting from medium to high current densities, as presented in Fig. ~~5~~ 4. It can be noticed that the geometrical effect on the performance is a function of the operating conditions: at low current densities the channels width effect is negligible; at medium current densities, the improved electrical contact between the flow field plates and GDLs, as presented in Table 3, leads to a reduction in the ohmic losses and consequently to an increase in performance; while at high current densities, where more liquid water is produced, the influence of decreasing the channels width become more significant. By decreasing the channel width, the gas velocity increases, facilitating the liquid water removal; see Fig. ~~6~~ 5 which shows that water saturation is maximum for the case with 14-channels serpentine. As a consequence, the transport of oxygen will not be obstructed and the increase in performance in the mass transport losses region is explained. The results are in accordance with those found in ~~[35]~~ [41].

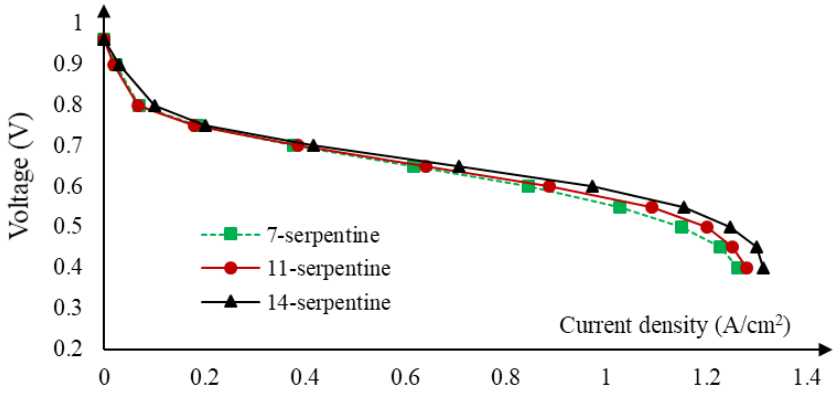

Fig. ~~5~~ 4 - Polarization curves for various patterns of the flow channels.

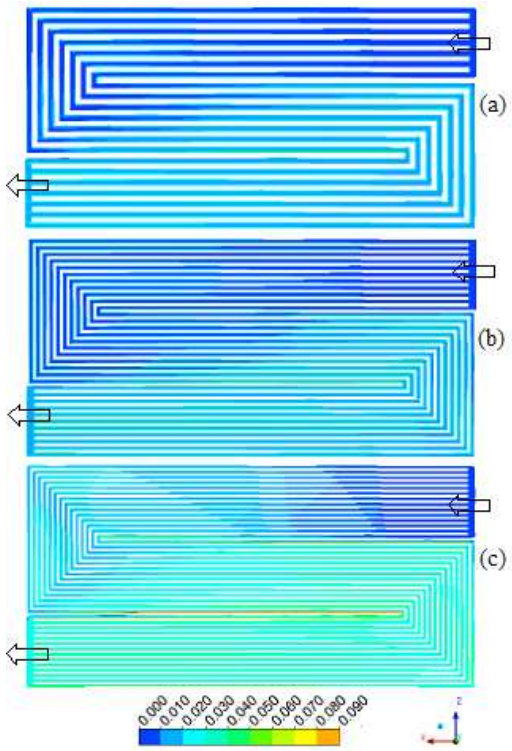

Fig. ~~6~~ 5 – Liquid water saturation at the mid-thickness of the cathode channel for the PEM fuel cell with:7-channels serpentine, (b) 11-channels serpentine, and (c) 14- channels serpentine.

The flow-field plate with 14-serpentine channels showed the best performance. This configuration has been manufactured and experimentally tested using an in-house fuel cell test station, and has been used to further analyse the impact of the channel depth variation on the fuel cell performance. The influence of the air flow rate on the fuel cell performance has also been studied based on this configuration.

3.3. Influence of the flow field depth

The 14-channels serpentine fuel cell has been used to investigate the channel depth influence on the performance and on the mass transport related parameters. For a given channel width of 1.2 mm, 4 geometries with various depths have been considered, namely: 0.25 mm, 0.4 mm, 0.6 mm and 0.8 mm. Smaller channel depths are required to have lighter bipolar plates and to make fuel cell stacks integration possible in applications that requires low volume and weight, such as portable applications. The polarization curves are obtained after running numerical simulations for each case taking a potential difference between the anode and the cathode in the range 0.962-0.4V; the results are presented in Fig. ~~7~~ 6. The findings show that the current density increases by 7% by decreasing the channel depth from 0.8 mm to 0.25 mm at 0.4V.

It is known that a critical challenge for the design of the flow fields and bipolar plates is to ensure an appropriate water management [11, 27] and reactant transport; therefore, the channels should effectively remove the accumulated water to avoid the flooding problem and at the same time allow the reactants to reach the catalyst layers where the electrochemical reactions occur. It is important to decrease the parasitic losses which are directly linked to the pressure drop along the channels. A higher pressure drop can effectively eliminate the water accumulated in the flow channels, but demands higher pumping power. The ideal flow field is expected to overcome the problem of flooding at as low pressure drop as possible. The multiple-serpentine flow channels have a pressure drop greater than the other types of channels due to the large length of the channel and the many turns that the flow makes. Although the water produced is removed efficiently, the outlet regions can be prone to flooding and the membrane can dehydrate in the inlet region for the serpentine configuration, as can be seen in Fig.

~~8~~ 7. Managing the membrane water content is a requirement for ensuring a high protonic conductivity since a well humidified membrane will allow the protons to pass through and reduce the ohmic losses.

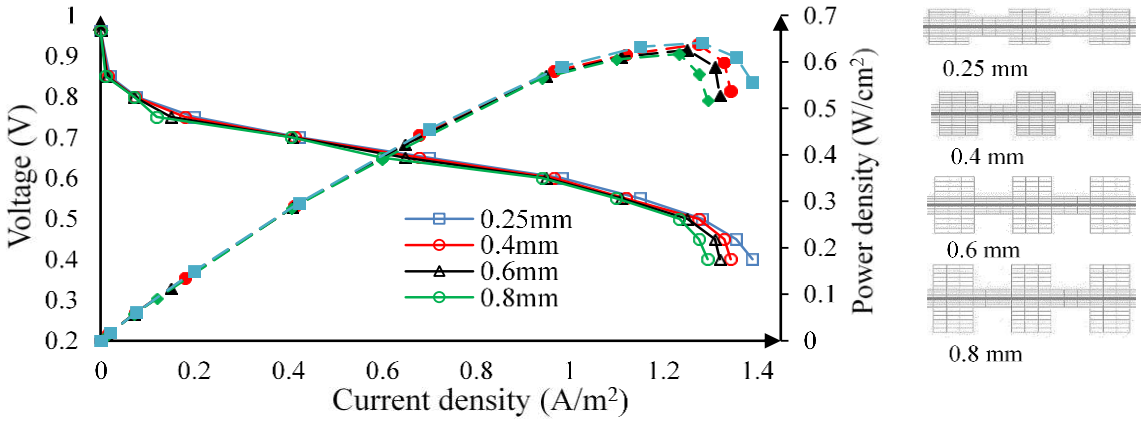

Fig. ~~7~~ 6 Polarization curves for different channel depths.

At high current densities, a large amount of water is produced and this tends to accumulates in the channels, so the pressure drop become the most important factor in the elimination of the excess water and in facilitating the transport of oxygen. The polarization curves, presented in Fig. ~~7~~ 6, shows that the best performance is achieved at the smallest channel depth (0.25 mm) investigated. The pressure drop for each case, using the same boundary conditions, is reported for the anode and cathode channels, see Table 4. It can be noticed that there is a significant increase in the pressure drop as the channel depth decreases; the results are in accordance with the findings of several studies [7-10].

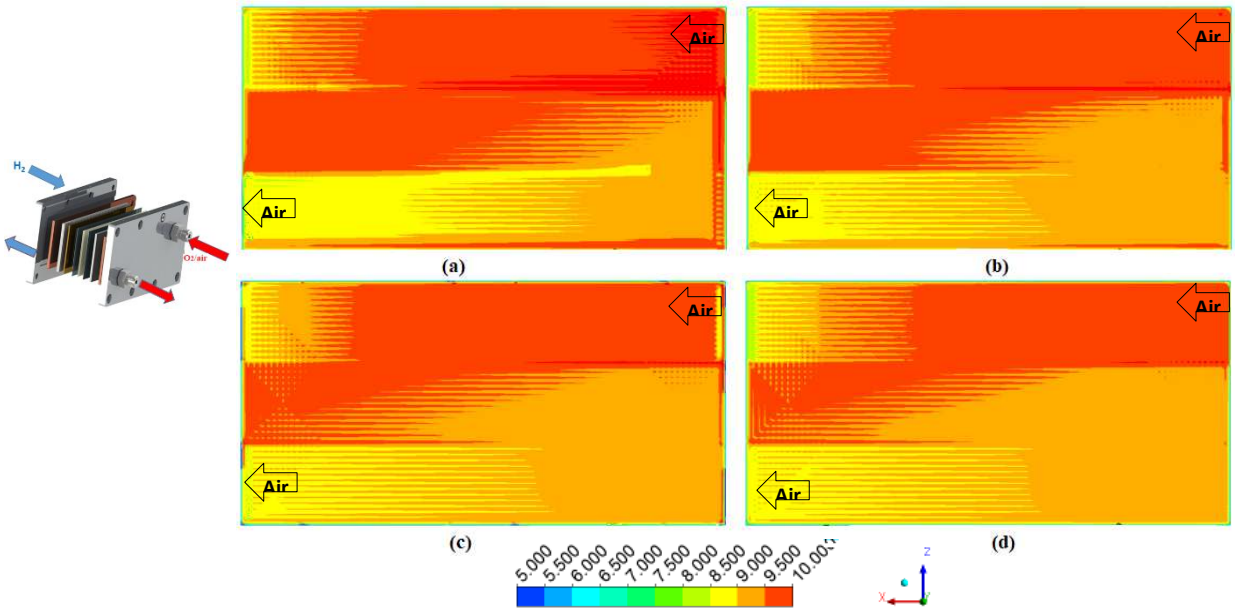

Fig. ~~8~~ 7 – Profiles of the water content at the interface between the ~~anodic~~ cathodic CL and membrane at 0.6 V with different channel depths: (a) 0.25 mm, (b) 0.4 mm, (c) 0.6 mm and (d) 0.8 mm.

Table 4 Maximum Pressure drop reported in PEM fuel cell channels.

Channel Depth	Pressure drop in anode channel	Pressure drop in cathode channel
0.8 mm	368 Pa	1327 Pa
0.6 mm	683 Pa	2499 Pa
0.4 mm	1835 Pa	6509 Pa
0.25 mm	5254 Pa	17841 Pa

3.4. Influence of the air flow rate

One of the critical parameters for PEM fuel cell performance is the mass flow rate of the reacting gases ~~[25, 34]~~ [41-42]. As the mass flow rate of the air increases quadruples, the fuel cell perform significantly better and the distribution of the current density becomes more uniform; see Fig. ~~9~~ 8. This is due to the increased availability of oxygen for the electrochemical reactions (see Fig. ~~10~~ 9a) and the increased effectiveness of removal of water (see Fig. 9b). It could be clearly seen from the plots D in Fig. ~~10~~ 9a and Fig. ~~10~~ 9b that the highest amount of oxygen and the lowest amount of water at the interface between the cathode catalyst layer and the micro-porous layer are obtained for the maximum reported flow rate, i.e. 4 x 10^{-4} kg/s. Fig. 9c shows that difference between the flow rates of water entering and exiting the cathode flow channel slightly increases with increasing air flow rate, signalling that the less water is available at the cathode side with increasing air flow rate and confirming the contour plots presented in Fig. 9(b). These findings are in accordance with those of Yang et al. [46].

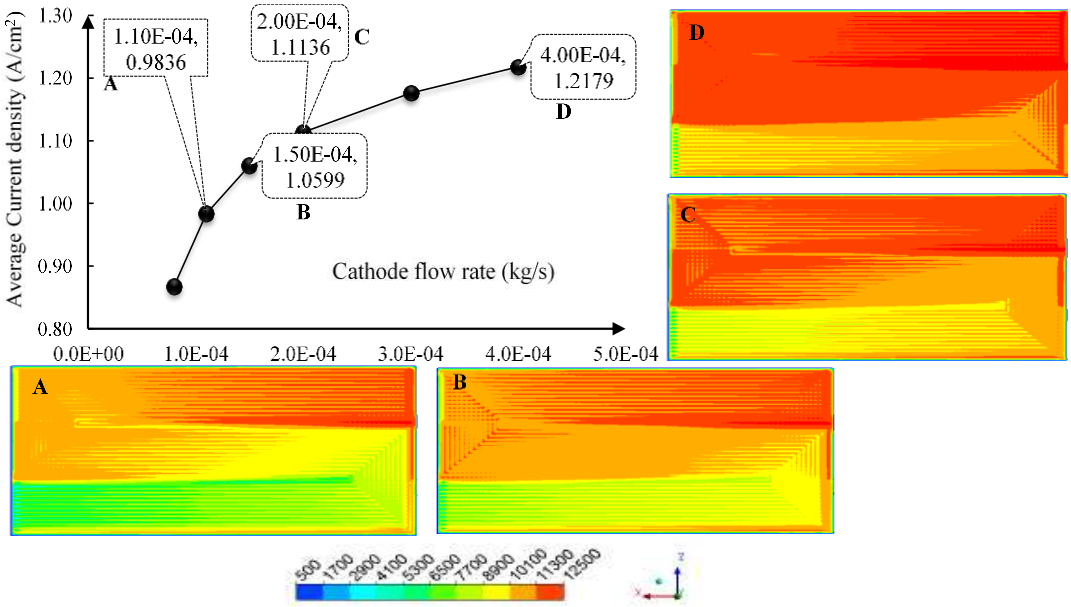

Fig. ~~9~~ 8 – Current density plot and profiles in the middle of the membrane for various air flow rates: (A) 1.1e-4 kg/s, (B) 1.5e-4 kg/s, (C) 2e-4 kg/s and (D) 4e-4 kg/s.

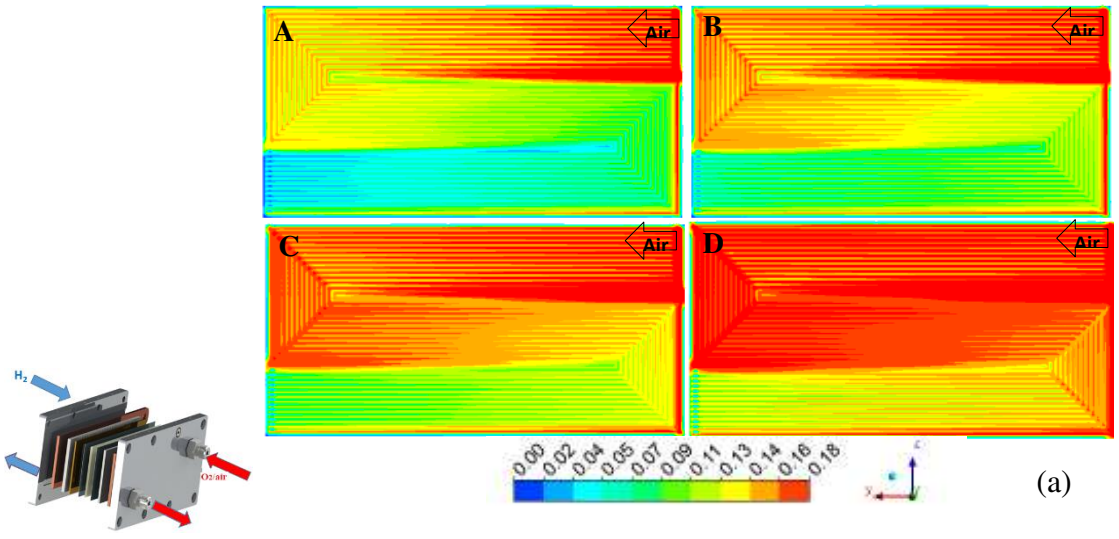

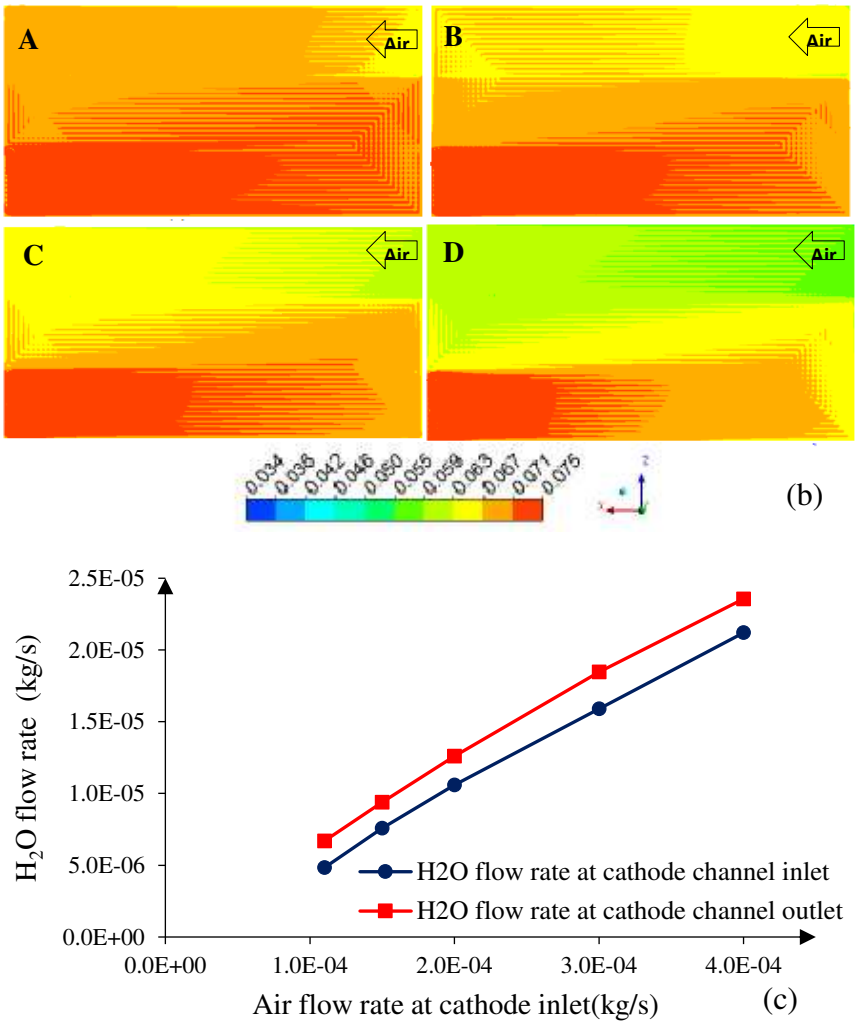

Fig. ~~10~~ 9 – (a) Oxygen mass fraction, (b) Water mass fraction profiles at the interface between the cathode CL and MPL at 0.6V for various air flow rates: (A) 1.1e-4, (B) 1.5e-4, (C) 2e-4 and (D) 4e-4 kg/s; and (c)Water flow rate at cathode channel inlet and outlet (kg/s) as a function of air flow rate (kg/s) at the cathode inlet.

4. Conclusions

A CFD model for a 200 cm² active area PEM fuel cell has been used to analyse the effect of the flow channels design on the fuel cell performance. To achieve this, different patterns and different cross-sectional dimensions have been investigated. The CFD results were in very good agreement with the experimental data obtained from the fuel cell run with the 14-channels serpentine (base case – channels with 0.6 mm width). The main results of the investigation are summarized as follows:

(i) As the number of channels of the serpentine configuration increases from 7 to 14 (or as the channel width-to-land width ratio decreases), the fuel cell performs better, especially at the high current densities. This is attributed to the improved electrical contact between the flow-field plates and the GDLs and the increased rate of supply of reacting gases to the active area in CLs. An increase of 5% in the contact area between bipolar plate and GDL leads to an increase of 15% in current density at 0.6V.

(ii) For the optimised flow field design (i.e. 14-channels serpentine flow field), as the channel depth decreases from 0.8 mm to 0.25 mm, the current density increases up to around 7%. The decrease in the depth of the channel increases the convective flow in the channels, facilitating the removal of excess liquid water.

(iii) As the air flow rate increases, the fuel cell performance improves and this is due to the increased supply rate of oxygen and increased removal rate of excess water. The current density increases by about 25% when increasing the air flow rate by a factor of 4.

Acknowledgements

This work was supported by a grant from the Romanian Ministry of Research and Innovation, CCCDI - UEFISCDI, project no. PN-III-P1-1.2-PCCDI-2017-0194/25 PCCDI within PNCDI III.

References

[1] https://www.fch.europa.eu/page/fch-ju-projects
[2] Wang J. Barriers of scaling-up fuel cells: Cost, durability and reliability. Energy 2015; 80: 509-21, https://doi.org/10.1016/j.energy.2014.12.007.
[3] Xu Y, Peng L, Yi P, Lai X. Analysis of the flow distribution for thin stamped bipolar plates with tapered channel shape. Int J Hydrogen Energy 2016; 41(9): 5084-95, https://doi.org/10.1016/j.ijhydene.2016.01.073.
[4] Kahraman H, Orhan M.F. Flow field bipolar plates in a proton exchange membrane fuel cell: Analysis & modelling. Energy Convers Manag 2017; 133:363-84, https://doi.org/10.1016/j.enconman.2016.10.053.
[5] Kone JP, Zhang X, Yan Y, Hu G, Ahmadi G. Three-dimensional multiphase flow computational fluid dynamics models for proton exchange membrane fuel cell: A theoretical development. J Comput Multiph Flows. 2017; 9(1): 3–25, https://doi.org/10.1177/1757482X17692341.
[6] Shimpalee S, Greenway S, Van Zee JW. The impact of channel path length on PEMFC flow-field design. J Power Sources 2006; 160: 398-406, https://doi.org/10.1016/j.jpowsour.2006.01.099.
[7] Kerkoub Y, Benzaoui A, Fadila Haddad, Yasmina K. Ziari. Channel to rib width ratio influence with various flow field designs on performance of PEM fuel cell. Energy Convers Manag 2018; 174: 260–75, https://doi.org/10.1016/j.enconman.2018.08.041.
[8] Wilberforce T, Hassan ZE, Ogungbemi E, Ijaodola O, Khatib FN, Durrant A, Thompson J, Baroutaji A, Olabi A.G. A comprehensive study of the effect of bipolar plate (BP) geometry design on the performance of proton exchange membrane (PEM) fuel cells. Renew Sustain Energy Rev 2019; 111: 236-60, https://doi.org/10.1016/j.rser.2019.04.081.
[9] Manso AP, Marzo FF, Barranco J, Garikano X, Garmendia Mujika M. Influence of geometric parameters of the flow fields on the performance of a PEM fuel cell. A review. Int J Hydrogen Energy 2012; 37: 15256-87, 10.1016/j.ijhydene.2012.07.076.
[10] Choi K-S, Kim H-M, Moon S-M. Numerical studies on the geometrical characterization of serpentine flow-field for efficient PEMFC. Int J Hydrogen Energy 2011; 36(2): 1613-27, https://doi.org/10.1016/j.ijhydene.2010.10.073.
[11] Spernjak D, Prasad A, Advani S. In situ comparison of water content and dynamics in parallel, single-serpentine, and interdigitated flow fields of polymer electrolyte membrane fuel cells. J Power Sources 2010; 195: 3553-68, https://doi.org/10.1016/j.jpowsour.2009.12.031.
[12] Shimpalee S, Vanzee J. Numerical studies on rib & channel dimension of flow field on PEMFC performance. Int J Hydrogen Energy 2007; 32 (7): 842-56, https://doi.org/10.1016/j.ijhydene.2006.11.032.
[13] Hashemi F, Rowshanzamir S, Rezakazemi M, CFD simulation of PEM fuel cell performance: Effect of straight and serpentine flow fields. Mathematical and Computer Modelling 2012; 55: 1540–57, https://doi.org/10.1016/j.mcm.2011.10.047.
[14] Li WZ, Yang WW, Zhang WY, Qu Z.G, He Y.L. Three-dimensional modeling of a PEMFC with serpentine flow field incorporating the impacts of electrode inhomogeneous compression deformation. Int J Hydrogen Energy 2019; 44(39): 22194-209, https://doi.org/10.1016/j.ijhydene.2019.06.187.
[15] Lee S, Kim T, Park H. Comparison of multi-inlet and serpentine channel design on water production of PEMFCs. Chem Eng Sci, 2011; 66: 1748-58, https://doi.org/10.1016/j.ces.2011.01.007.
[16] Park J, Li X. An experimental and numerical investigation on the cross flow through gas diffusion layer in a PEM fuel cell with a serpentine flow channel. J Power Sources, 2007; 163: 853-63, https://doi.org/10.1016/j.jpowsour.2006.09.083.
[17] Ram Kumar R,Suresh S, Suthakar T , Kumar Singh V. Experimental investigation on PEM fuel cell using serpentine with tapered flow channels. Int J Hydrogen Energy, 2020; 45(31): 15642-9, https://doi.org/10.1016/j.ijhydene.2020.04.023.

[18] Wang J.Y. Pressure drop and flow distribution in parallel-channel configurations of fuel cells: U-type arrangement. Int J Hydrogen Energy 2008; 33(21): 6339-50, https://doi.org/10.1016/j.ijhydene.2008.08.020.
[19] Carcadea E, Varlam M, Ingham DB, Ismail MI, Patularu L, Marinoiu A, Schitea D. The effects of cathode flow channel size and operating conditions on PEM fuel performance: A CFD modelling study and experimental demonstration. Int J Energy Res 2018; 42(8); 2789-804, https://doi.org/10.1002/er.4068.
[20] Lim BH, Majlan EH, Daud WRW, Rosli MI, Husaini T. Numerical investigation of the effect of three-dimensional modified parallel flow field designs on proton exchange membrane fuel cell performance. Chem Eng Sci 2020; 217 115499, https://doi.org/10.1016/j.ces.2020.115499.
[21] Santamaria AD, Cooper NJ, Becton MK, Park JW. Effect of channel length on interdigitated flow-field PEMFC performance: A computational and experimental study. Int J Hydrogen Energy 2013; 38(36): 16253-63, https://doi.org/10.1016/j.ijhydene.2013.09.081.
[22] Liu H, Li P, Juarez-Robles D, Wang K. Experimental Study and Comparison of Various Designs of Gas Flow Fields to PEM Fuel Cells and Cell Stack Performance. Front Energy Res, 2014; 2, article 2 10.3389/fenrg.2014.00002, doi: 10.3389/fenrg.2014.00002.
[23] Perng S-W, Wub H-W, Wang R.-H. Effect of modified flow field on nonisothermal transport characteristics and cell performance of a PEMFC. Energy Convers Manag, 2014; 80: 87-96, https://doi.org/10.1016/j.enconman.2013.12.044.
[24] Limjeerajarus N, Santiprasertkul T. Novel hybrid serpentine-interdigitated flow field with multi-inlets and outlets of gas flow channels for PEFC applications. Int J Hydrogen Energy, 2020; 45(25): 13601-11, https://doi.org/10.1016/j.ijhydene.2018.12.160.
[25] Wilberforce T, Khatib FN, Ijaodola OS, Ogungbemi E, El-Hassan Z, Durrant A, Thompson J, Olabi AG. Numerical modelling and CFD simulation of a polymer electrolyte membrane (PEM) fuel cell flow channel using an open pore cellular foam material. Sci Total Environ, 2019; 678: 728–40, https://doi.org/10.1016/j.scitotenv.2019.03.430.
[26] Baroutaji A, Carton JG, Stokes J, Olabi AG. Application of Open Pore Cellular Foam for air breathing PEM fuel cell. Int J Hydrogen Energy 2017; 42(40): 25639-62, https://doi.org/10.1016/j.ijhydene.2017.05.114.
[27] Hsieh SS, Bing-Shyan H, Huang C-J. Effect of pressure drop in different flow fields on water accumulation and current distribution for a micro PEM fuel cell. Energy Convers Manag. 2011; 52: 975-82, https://doi.org/10.1016/j.enconman.2010.08.025.
[28] Baek SM, Yu SH, Nam JH, Kim C.-J. A numerical study on uniform cooling of large-scale PEMFCs with different coolant flow field designs. Appl Therm Eng. 2011; 31(8): 1427-34, https://doi.org/10.1016/j.applthermaleng.2011.01.009.
[29] Shimpalee S, Hirano S, DeBolt M, Lilavivat V, Weidner JW, Khunatornb Y, Macro-Scale Analysis of Large Scale PEM Fuel Cell Flow-Fields for Automotive Applications. J Electrochem Soc. 2017; 164 (11): E3073-E3080, DOI: 10.1149/2.0091711jes.
[30] Abdulla S, Patnaikuni VS. Performance evaluation of Enhanced Cross flow Split Serpentine Flow Field design for higher active area PEM fuel cells. Int J Hydrogen Energy. 2020, 10.1016/j.ijhydene.2020.01.199.
[31] Vijayakrishnan MK, Palaniswamy K, Ramasamy J, Kumaresan T, Manoharan K, Rajagopal TKRR, Maiyalagan T, Jothi VR, Yi S-C. Numerical and experimental investigation on 25 cm^2 and 100 cm^2 PEMFC with novel sinuous flow field for effective water removal and enhanced performance. Int J Hydrogen Energy 2020; 45(13): 7848-62, DOI: 10.1016/j.ijhydene.2019.05.205.
[32] Li X, Sabir I, Park J. A flow channel design procedure for PEM fuel cells with effective water removal. J Power Sources. 2007; 163 (2): 933-42, https://doi.org/10.1016/j.jpowsour.2006.10.015.
[33] Lakshminarayanan V, Karthikeyan P. Performance enhancement of interdigitated flow channel of PEMFC by scaling up study. Energy Sources, Part A: Recovery, Utilization, and Environmental Effects. 2020; 42(14): 1785-96, https://doi.org/10.1080/15567036.2019.1604889.
[34] Cha SW, O'Hayre R, Saito Y, Prinz F.B. The scaling behavior of flow patterns: a model investigation. J Power Sources 2004; 134 (1):57-71.
[35] Peng L, Shao H, Qiu D, Yia P, Lai X. Investigation of the non-uniform distribution of current density in commercial-size proton exchange membrane fuel cells. J Power Sources. 2020; 453: 227836, https://doi.org/10.1016/j.jpowsour.2020.227836.

[36] Carcadea E, Varlam M, Ismail MS, Ingham DB, Marinoiu A, Raceanu M, Jianu C, Patularu L, Ion-Ebrasu D. PEM fuel cell performance improvement through numerical optimization of the parameters of the porous layers. Int J Hydrogen Energy 2020; 45(14): 7968-80, https://doi.org/10.1016/j.ijhydene.2019.08.219.
[37] Berning T, Djilali N. A 3D, multiphase, multicomponent model of the cathode and anode of a PEM fuel cell. J Electrochem Soc 2003; 150: A1589 -98.
[38] Barbir F. PEM Fuel Cell: Theory and Practice. Amsterdam; Boston: Elsevier Academic Press; 2012.
[39] Wilberforce T, Hassan ZE, Khatib FN, Makky AA, Mooney J, Baroutaji A, Carton JG. Development of Bi-polar plate design of PEM fuel cell using CFD techniques. Int J Hydrogen Energy 2017; 42 (40): 25663-85, https://doi.org/10.1016/j.ijhydene.2017.08.093.
[40] ANSYS. Multiphysics help, www.ansys.com, Chapter 33: Modeling Fuel cells
[41] Sadiq Al-Baghdadi MAR, Shahad Al-Janabi HAK. Modeling optimizes PEM fuel cell performance using three-dimensional multi-phase computational fluid dynamics model. Energy Convers Manag. 2007; 48 (12): 3102-19, https://doi.org/10.1016/j.enconman.2007.05.007.
[42] Pierre JS, Wilkinson D, Knights S. Relationships between water management contamination and lifetime degradation in PEMFC. J New Mater Electrochem Syst 2000; 3:99–106.
[43] Wei-Mon Y, Yang C-H, Chyi-Yeou S, Chen F, Sheng-Chin M. Experimental studies on optimal operating conditions for different flow field designs of PEM fuel cells. J Power Sources 2006; 160: 284-92, https://doi.org/10.1016/j.jpowsour.2006.01.031.
[44] J. Park, X. Li. An experimental and numerical investigation on the cross flow through gas diffusion layer in a PEM fuel cell with a serpentine flow channel. J Power Sources, 163 (2007), pp. 853-863
[45] Pourya KT, Ehsan SN, Mohsen G Numerical and experimental investigation on effects of inlet humidity and fuel flow rate and oxidant on the performance on polymer fuel cell, Energy Convers Manag. 2016; 114:290-302, https://doi.org/10.1016/j.jpowsour.2006.09.083.
[46] Yang Z, Du Q, Jia Z, Yang C, Jiao K. Effects of operating conditions on water and heat management by a transient multi-dimensional PEMFC system model. Energy 2019; 183: 462–76, https://doi.org/10.1016/j.energy.2019.06.148.